VANE DEMISTER PROJECT

Andrew Simon, Angela Maio, Adam Hutchinson, Vineet Padia

MAY 2, 2015

SECTION 0104 TEAM 2

Table of Contents

Introduction

In many industrial applications, it is often necessary to process fluids in order to separate liquid components from gaseous components. This separation provides a means to control the quality of the fluid and several other dependent parameters including enthalpy and pressure. In some cases, the presence of liquids in industrial fluid flow can not only reduce efficiency but cause system component damage.

To demonstrate the importance of this problem, consider the problem of a salt water distillation facility. These types of facilities convert impure seawater, containing salts and other contaminants, to potable water. In some desalination plants, the intake seawater is heated rapidly and converted to a vapor. While many of the solutes are left behind in solid form, the quality of the vapor is not 100%. Some of the particulate solutes are still contained within the liquid portion of the vapor. To achieve a higher separation efficiency, it is necessary to remove this contaminated liquid from the outgoing fluid. The gaseous component is pure and, once condensed, useable as potable drinking water.

In this study, there are several specific objectives that are to be accomplished.

1. A simulation code will be developed that models a vane-impactor demister system for a scaled model facility.
2. For both the model facility and prototype scale, the 90% critical droplet diameter will be calculated.
3. Using an appropriate scaling and nondimensionalization, the results of the simulated system will be applied to predict the function of a prototype demister. These results will be compared to the behavior from the simulated prototype.

To achieve these goals, dimensionless pi terms are calculated using the Buckingham Pi Theorem. The most important parameters and pi terms are chosen; these are used to determine the scale of the prototype demister and whether tests with the prototype will be accurate enough in predicting how the system will behave.

Discussion of Physical Phenomena

This type of demister works in the following manner: An incoming mist flow is funneled into the device. The fluid is forced around a series of circular vanes, which deform the streamlines significantly. Suspended droplets in the flow are swept along with the fluid, but also carry some preexisting inertia which attempts to carry the droplets in a straight line. Although the fluid has a drag force large enough to effect the curved motion of the droplets, the inertial component of motion may cause the path of the particles to deviate far enough to intersect with the vanes. The droplets are thus removed from the flow by direct impact, meaning the droplet hits the surface of the vane and stops so that it is no longer a part of the fluid flow (“Demisters to Remove Fine Droplets of Liquid,” 2015). This effect is more pronounced with larger droplets, as they will be less affected by the surrounding fluid due to their larger mass. As the streamlines are location-dependent, so too is the rate of droplet collection. Some droplets that start their path through the demister will not collide with any vanes and continue in the output fluid flow. The velocity of the fluid flow also affects the demister’s collection efficiency since it affects the path the droplets will follow through the vanes (Gharib and Moraveji, 2015). We considered these parameters

when determining how to simulate the flow of droplets through the curved vane demister to determine the critical droplet size for a 90% collection efficiency for a model and prototype scale.

Dimensional Analysis

Selection of parameters requires a working knowledge of the phenomenon involved and the governing physical laws of the model. The phenomenon involved in this model is the mechanical removal of particles through inertial separation. The heavier contaminating particles cannot turn as quickly as the gas, and therefore collide with the vane impactors.

The dimensional parameters used to determine particle motion were divided into three subgroups for better organization. These subgroups include geometry, material properties, and external effects. Geometric dimensional parameters considered include vane radius of curvature, vane horizontal spacing, channel gap width, width of vanes, droplet diameter. Some important material properties for the model include atmospheric density, droplet density, and the atmospheric dynamic viscosity. External effect parameters include collection efficiency, total pressure drop, drag force, and the relaxation time. Based on the physical phenomenon these parameters were most important for model the demister.

Table 1: Dimensional parameters and associated pi terms

Var No.	Symbol	Description	Dimension	Pi Group	Constraint
1.	η	Collection Efficiency	None	$\Pi_1 = \eta$	Dependent
2.	F_d	Drag Force	MLT^{-2}	$\Pi_2 = \frac{F_d}{\rho_g V_g{}^2 D^2}$	Dependent
3.	t	Relaxation Time (const in decay of droplet velocity)	T	$\Pi_8 = \frac{\mu_g t}{D^2 \rho_d}$	Dependent
4.	R	Vane Radius of Curvature	L	$\Pi_3 = \frac{R}{D}$	Independent
5.	H	Vane Horizontal Spacing	L	$\Pi_4 = \frac{H}{D}$	Independent
6.	L	Channel Gap Width	L	$\Pi_5 = \frac{L}{D}$	Independent
7.	ρ_d	Droplet Density	ML^{-3}	$\Pi_6 = \frac{\rho_d}{\rho_g}$	Independent
8.	μ_g	Gas Dynamic Viscosity	$ML^{-1}T^{-1}$	$\Pi_7 = \frac{\rho_g V_g R}{\mu_g}$	Fixed
9.	V_g	Upstream gas velocity	LT^{-1}	Repeating	Fixed
10.	D	Droplet diameter	L	Repeating	Fixed
11.	ρ_g	Gas Density	ML^{-3}	Repeating	Fixed
12.	g	Gravitational Acceleration	LT^{-2}	$\Pi_9 = \frac{V_f}{\sqrt{gL}}$	Independent

Analytical Model Development

Using the dimensional parameters from the previous section, an analysis of the external forces acting on the droplets can be performed. The forces are shown below in the free body diagram.

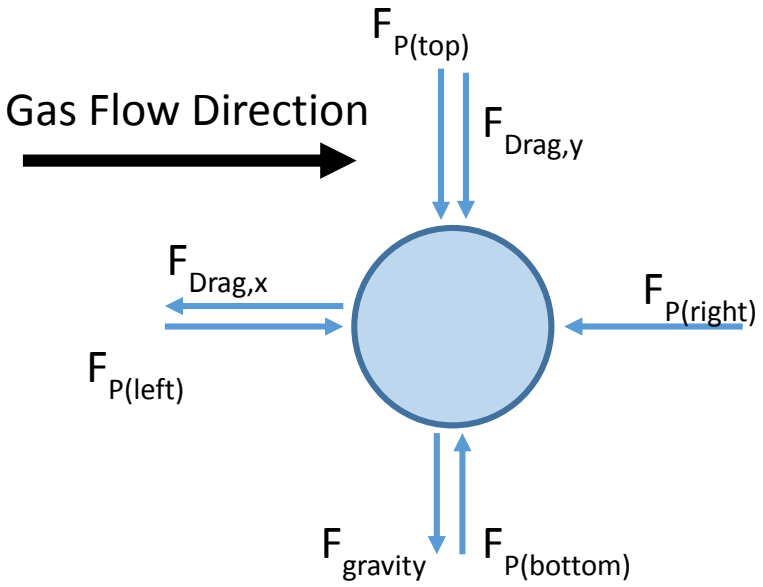

Figure 1: Free body diagram of a water droplet flowing through the demister

From the sum of the forces illustrated in the free body diagram, the following equations were used to obtain the equations of motion for the particle with a variable fluid velocity.

$$\sum F_x = ma_x = F_{P(left)} - F_{P(right)} + F_{Drag,x} = \frac{\rho_d \pi D^3}{6}\frac{dV_x}{dt}$$

$$\sum F_y = ma_y = F_{P(bottom)} - F_{P(top)} - F_{gravity} - F_{Drag,y} = \frac{\rho_d \pi D^3}{6}\frac{dV_y}{dt}$$

$\vec{F}_{Drag} = C_d \frac{1}{2}\rho A \left(\overrightarrow{V_f} - \frac{dx_p}{dt}\right)\left|\overrightarrow{V_f} - \frac{dx_p}{dt}\right|$ and $F_p = pA$ are defined, which provides the following equations for motion in the x and y directions, respectively:

$$\frac{\rho_d \pi D^3}{6}\frac{dV_x}{dt} = p_{left}A - p_{right}A + C_d \frac{1}{2}\rho_d A\left(u_f - \frac{dx_p}{dt}\right)\sqrt{\left(u_f - \frac{dx_p}{dt}\right)^2 + \left(v_f - \frac{dy_p}{dt}\right)^2}$$

$$\frac{\rho_d \pi D^3}{6}\frac{dV_y}{dt} = p_{bottom}A - p_{top}A - mg - C_d \frac{1}{2}\rho_d A\left(v_f - \frac{dy_p}{dt}\right)\sqrt{\left(u_f - \frac{dx_p}{dt}\right)^2 + \left(v_f - \frac{dy_p}{dt}\right)^2}$$

Further, recognize that the pressure drops across the top/bottom and left/right of the particle are so small that they are negligible. This makes the pressure terms cancel each other out in both equations. As a result, the equations above can be simplified to:

$$\frac{\rho_d \pi D^3}{6}\frac{dV_x}{dt} = C_d \frac{1}{2}\rho_d A\left(u_f - \frac{dx_p}{dt}\right)\sqrt{\left(u_f - \frac{dx_p}{dt}\right)^2 + \left(v_f - \frac{dy_p}{dt}\right)^2}$$

$$\frac{\rho_d \pi D^3}{6}\frac{dV_y}{dt} = -mg - C_d \frac{1}{2}\rho_d A\left(v_f - \frac{dy_p}{dt}\right)\sqrt{\left(u_f - \frac{dx_p}{dt}\right)^2 + \left(v_f - \frac{dy_p}{dt}\right)^2}$$

Significance and Interpretation of Pi terms

Table 2: Pi terms and their importance to the problem

Pi Term	Definition	Description	Similitude Importance
Π_1	η	The main dependent variable being measured, this pi group designates the percentage of particles that continue through the entire demister without a collision.	The similitude of this pi term is one to one. We want the model's efficiency to match that of the prototype.
Π_2	$\frac{F_d}{\rho_g V_g^2 D^2}$	This term defines the relationship between the drag force, the initial kinetic energy of the fluid, and the oncoming surface area of the droplet. This pi term actually defines the Drag Coefficient.	The drag force is important to consider as it directly affects the motion of the particle. Further, there is a strong dependence on the upstream velocity and droplet diameter.
Π_3	$\frac{R}{D}$	The ratio of the vane radius to the droplet diameter will affect the available relative surface area on the vane that the droplet has to collide with. This ratio should be large to facilitate significant droplet removal.	It is nonessential to maintain exact proportionality between the vane radius and the droplet diameter, but rather an order of magnitude scaling.
Π_4	$\frac{H}{D}$	Streamwise element spacing relative to the droplet diameter gives a measure of how quickly the particle must overcome its inertia in order to follow the fluid flow.	Similar to Pi 3, this number will be large and it is only necessary to conserve the order of magnitude ratio.
Π_5	$\frac{L}{D}$	Vane spacing, relating linearly to the droplet diameter, directly affects the motion of the droplet through the pressure variation in the fluid. With a larger spacing, there can be a greater pressure difference between the elements and the center streamline. This pressure difference provides the force to adjust the path of the droplet.	See Pi 3
Π_6	$\frac{\rho_d}{\rho_g}$	The relative ratios of the droplet density and the gas density dictate how differently the droplets act than the rest of the fluid. As this ratio becomes larger, the droplets behave less like other fluid particles and have higher inertia when traveling along the streamline.	See Pi 3
Π_7	$\frac{\rho_g V_g R}{\mu_g}$	This term is the ratio of the inertial forces to viscous forces in the fluid, also known as the Reynolds number. It gives a measure of how turbulent or laminar the flow is around the vanes.	It is important to consider the similitude of the Reynolds Number, but it is not required to be one to one. As long as the prototype and model share turbulence or laminar characteristics, the similitude is sufficient.
Π_8	$\frac{\mu_g t}{D^2 \rho_d}$	Combined with Pi 8 and Pi 6, the Stokes number arises. Particles with a low Stk follow streamlines well while those with large Stk tend to continue along their initial trajectory.	The Stokes number should maintain a unity similitude between model and prototype. This will ensure that proportionally sized particles follow similar paths, and thus conserve the collection efficiency.
Π_9	$\frac{V_f}{\sqrt{gL}}$	This term is the ratio of kinetic energy to potential energy, or of flow inertia to an external field, also known as Froude's number. Considering the gravity field, a high Froude's number would indicate that gravity has a negligible effect on the particle's trajectory.	As long as it is sufficiently large, then we can neglect the effects of gravity on the flow. The Froude number appears in our equation of motion and therefore has perfect scaling between model and prototype (1:1)

Sample Pi Term Calculation

$$\Pi_2 = \frac{V_f}{\sqrt{gL}} = \frac{LT^{-1}}{\sqrt{LT^{-2}L}} = \frac{LT^{-1}}{LT^{-1}} \quad (dimensionless)$$

Model scaling specification

This section describes our calculations of the scaling between our prototype and model simulations using our pi terms, including Froude's number, Stoke's number, and the drag force term.

Froude's number Π_9 is the most influential to our experiments. It can take a different form:

$$\frac{V_g}{\sqrt{\mathrm{gL}}} \cdot \frac{C}{t} = \frac{V_g}{g \times t}$$

where 't' is the droplet relaxation time.

The Stoke's number, Π_9 a term that represents the drag force, because upon removal of μ and replaced by $\frac{F}{V_{rel} \cdot d}$, $\frac{t\mu}{d^2 \rho_d}$ becomes:

$$\frac{t \cdot F_d}{D^3 \cdot \rho_w \cdot Vrel}$$

Froude number (modified, as suggested before) = $\frac{g \times t}{Vrel}$

Drag force term = $\frac{\mathrm{Cd}\ V_{rel}^2\ \rho_f\ 0.75}{\mathrm{D} \times \rho w} \cdot \frac{t}{V_{rel}} = \frac{6\ \mathrm{Fd}\ t}{\pi\ \mathrm{D}^3\ \mathrm{V_{rel}}\ \rho_d}$, since Cd = $\frac{\mathrm{F_d}}{\frac{1}{2} \cdot \frac{\pi}{4} d^2 \cdot \mathrm{V_{rel}^2} \rho_g}$

F_d is then replaced with $\mu \mathrm{V_{rel}} d$ giving a scaling term of $\frac{\mu\ t}{\mathrm{d}^2 \rho_d}$

The length ratio between model and prototype geometries, L/L_m is 4. The Froude number can be converted to $\frac{g\ t^2}{L}$, hence, t-ratio $= \sqrt{\mathrm{L\ ratio}} = 2$. Therefore, the μ ratio equals the ρ_d ratio and $\sqrt{\mathrm{t\ ratio}}$ = d-ratio, therefore, with t-ratio = 2, D-ratio = 1.41, then V_g ratio= 2.

Using the pi terms, especially the drag force term, Stoke's number, and Froude's number (pi terms 7 through 9), the scaling between the prototype and the model could be determined. The final scaling results are shown in the table below with calculated values in bold.

Table 3: Parameters and scaling between prototype and model

Var No.	Symbol	Description	Prototype	Model
1.	η	Collection Efficiency	**90%**	**91%**
2.	F_d	Drag Force	N/A	N/A
3.	t	Relaxation Time (const in decay of droplet velocity)	N/A	N/A
4.	R	Vane Radius of Curvature	0.02m	0.005m
5.	H	Vane Horizontal Spacing	0.08m	0.02m
6.	L	Channel Gap Width	0.03m	0.0075m
7.	ρ_d	Droplet Density	900kg/m^3	**1109.6kg/m^3**
8.	μ_g	Gas Dynamic Viscosity	1.46(10^{-5})kg/m*s	1.8(10^{-5})kg/m*s
9.	V_g	Upstream gas velocity	8m/s	**10.13m/s**
10.	D	Droplet diameter	**14.326microns**	**20.26 microns**
11.	ρ_g	Gas Density	4.16kg/m^3	1.2kg/m^3
12.	g	Gravitational Acceleration	9.8m/s^2	9.8m/s^2

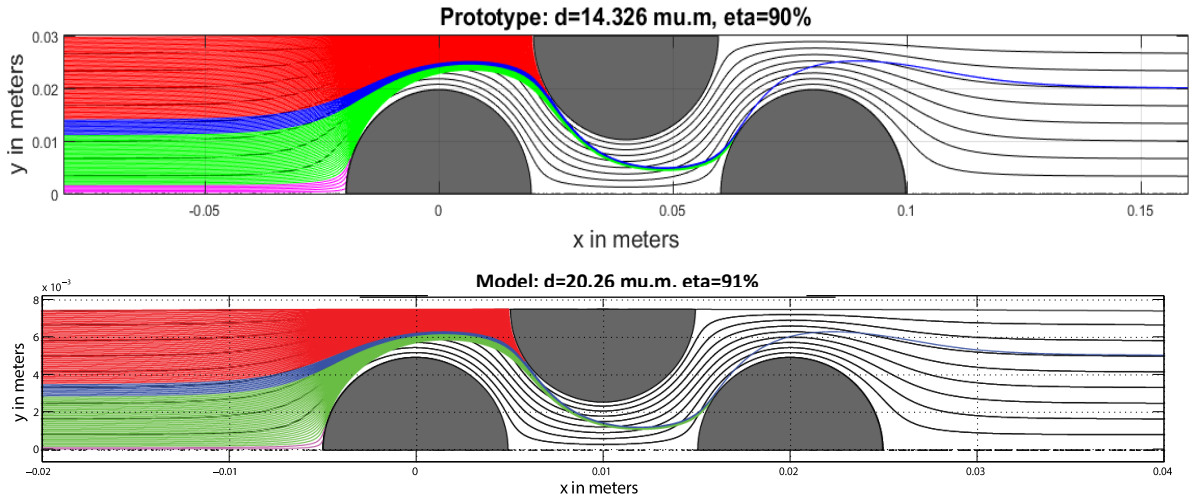

Figure 2: Prototype (top) and model (bottom) simulations displaying pathlines of escaping particles in blue and pathlines of particles that hit the first vane in pink, second vane in red, and third vane in green

Critical review of results

Using a MatLab simulation, the flow for both the prototype and model system was analytically computed. The program released a droplet of a specified size and location from the left side of the demister, and calculated its path as the gas flow carried it through the vanes. The simulation terminated if the droplet impacted on any of the three vanes, or if it passed through the system without colliding. By modeling the pathline for many droplets equally spaced along the demister intake and recording the number which impact versus the total number of droplets, the collection efficiency can be directly computed. Then this process can be iterated across many different droplet sizes to find the critical diameter, where a droplet with a random position has a 90% probability of being scrubbed from the flow. For expediency of calculation, a supercomputer (NIH BioWulf Cluster) was used for simulation.

In order to obtain values of particle density, particle diameter, and fluid velocity for our model, sacrifices to the obtained Reynolds number value obtained from the prototype have to be made. The model velocity can be varied between 0.1 to 50 meters per second. The Reynolds number determined by the prototype was 45000. Fluid velocity for the model corresponding to this Reynolds number is 136 meters per second which falls outside of the acceptable range. A Reynolds number of 2000 has a very similar drag coefficient to a Reynolds number of 45000 for a smooth sphere, as shown in the figure below (the relationship is linear for smaller values of Re). This justifies changing the Reynolds number from the prototype to the model to 2000, because it has minimal effect to the drag coefficient, and corresponds to an acceptable fluid velocity.

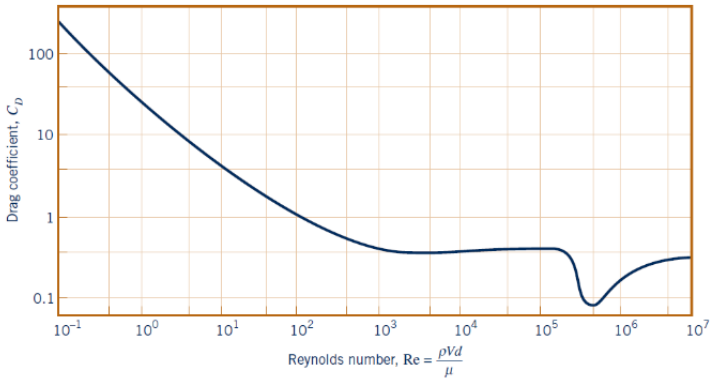

Figure 3: Effect of Reynolds number on the drag coefficient for a smooth sphere

Finishing out the rest of the dimensional analysis, a particle density of 1111 kg/m^3, a particle diameter of 20.26 microns and a fluid velocity of 6 meters per second were calculated using MatLab. Every value obtained fits within the model constraints, and these values obtained a similar collection efficiency to the prototype. The figure below displays the normalized velocity distribution when a test was run for the model. It shows where particles are stopped and collected by the vanes, as well as where they pass through at higher velocities.

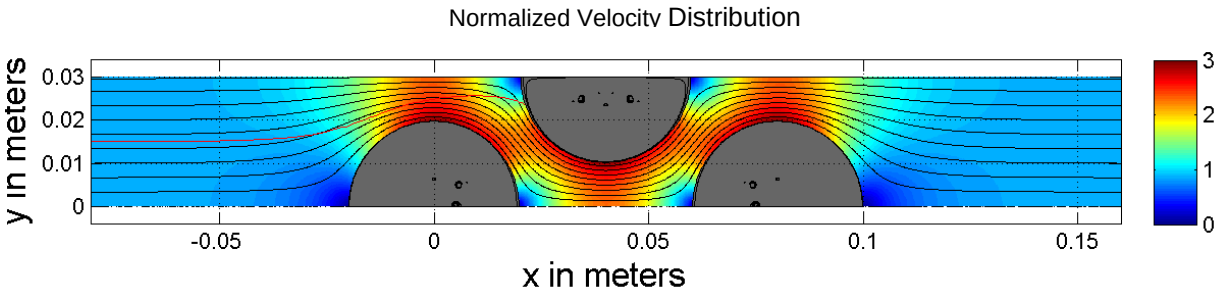

Figure 4: Model simulation showing the velocity distribution of the droplets in the fluid

Summary and Conclusions

In a droplet removal application, it was found that the corrugated vane impactor demister configuration functions very efficiently at removing liquids from a mist flow. A MatLab simulation was used to analyze the behavior of the suspended droplets in both the model geometry and the prototype geometry. A large number of droplet sizes were considered and analyzed to find the critical diameter at which 90% of droplets will be scrubbed from the fluid flow. Using nondimensional Pi term scaling analysis, the prototype critical droplet size was calculated numerically. It was shown that using a combination of the nondimensional scaling and simulation, the critical diameter for the prototype system and its operating conditions was determined.

This type of demister has several other advantages as well; since the fluid velocity is nearly equal on both sides of the device, there is only a small pressure drop through the entire flow. This minimizes the equipment necessary to pump the fluid through the device, which can aid in reducing project budget. Further, there are no moving parts within the device. This significantly diminishes the maintenance required for an industrial application.

Bibliography

"Demisters to Remove Fine Droplets of Liquid." Gaseous Emissions from Amine Based Post Combustion CO2 Capture Processes and Their Deep Removal (2012). IEA Greenhouse Gas R&D Programme. Web. 18 Apr. 2015.

Gharib, Jaber, and Mostafa Keshavarz Moraveji. "Determination the Factors Affecting the Vane-Plate Demisters Efficiency Using CFD Modeling." Journal of Chemical Engineering and Process Technology (2012). OMICS International. Web. 6 May 2015.

"Gas/Liquid Separators - Type Selection and Design Rules." Design and Engineering Practice (2007). Shell Global Solutions International. Web. 6 May 2015.

Kavousi, Fatemeh, Yaghoub Behjat, and Shahrokh Shahhosseini. "Optimal Design of Drainage Channel Geometry Parameters in Vane Demister Liquid–gas Separators." Chemical Engineering Research and Design 91.7 (2013): 1212-222. Science Direct. Web. 8 Apr 2015.

Munson, Bruce Roy, and T. H. Okiishi. Fundamentals of Fluid Mechanics. 7th ed. Hoboken, NJ: John Wiley & Sons, 2013. Print.

Venkatesan, G., N. Kulasekharan, and S. Iniyan. "Influence of Turbulence Models on the Performance Prediction of Flow through Curved Vane Demisters." Desalination 329 (2013): 19-28. Science Direct. Web. 6 May 2015.

Venkatesan, G., N. Kulasekharan, and S. Iniyan. "Numerical Analysis of Curved Vane Demisters in Estimating Water Droplet Separation Efficiency." Desalination 339 (2014): 40-53. Science Direct. Web. 6 May 2015.

Zhao, Jianzhi, Baosheng Jin, and Zhaoping Zhong. "Study of the Separation Efficiency of a Demister Vane with Response Surface Methodology." Journal of Hazardous Materials 147.1-2 (2007): 363-69. Science Direct. Web. 18 Apr. 2015.

Contributions

Adam Hutchinson – 19% External Research, Interpretation of Pi Terms, Report Editing

Angela Maio – 19% Pi Term construction, Preliminary Report, Equations of Motion Derivation, Discussion of Physical Phenomena

Vineet Padia – 43% Matlab simulation, Nondimensional Scaling Calculations, Plot Generation

Andrew Simon – 19% Final Report Introduction/Conclusion, Review of Results, Preliminary Report

Appendix

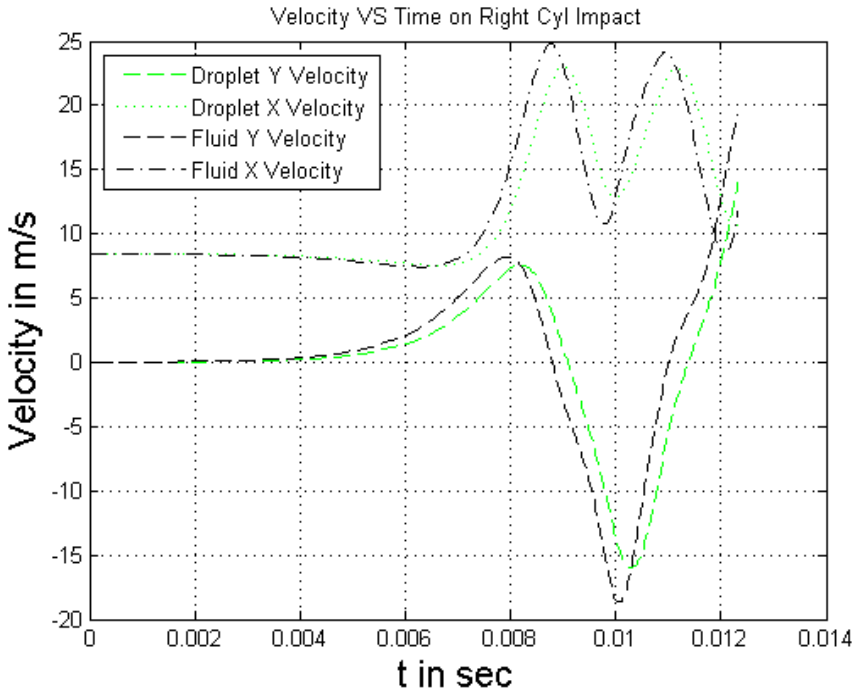

Shown above is the velocity profile with respect to time of a droplet (contaminant), and the surrounding fluid from an initial starting position to its point of impact (rightmost vane).

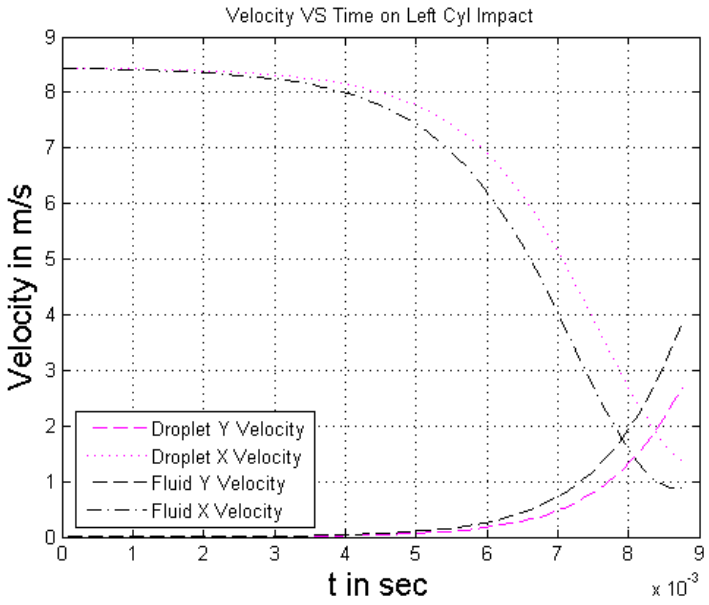

Shown above is the velocity profile with respect to time of a droplet (contaminant), and the surrounding fluid from an initial starting position to its point of impact (leftmost vane).

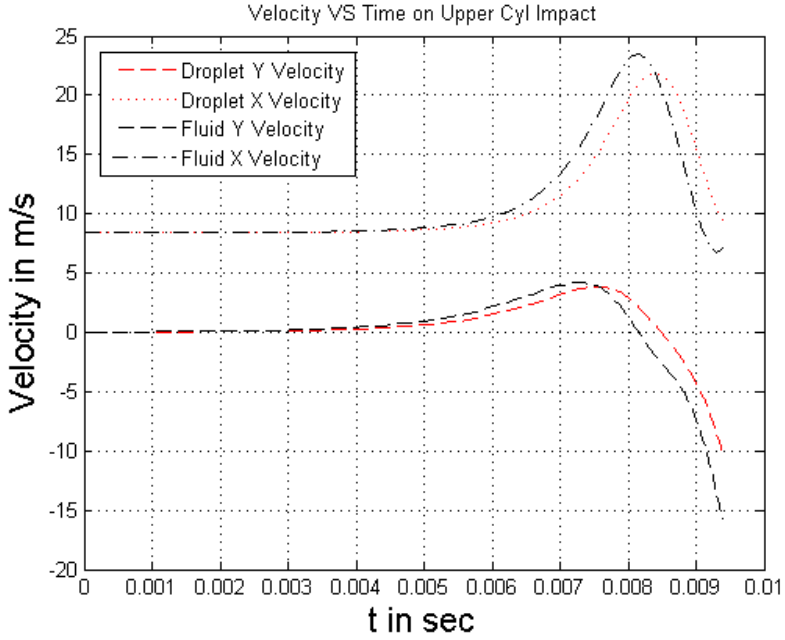

Shown above is the velocity profile with respect to time of a droplet (contaminant), and the surrounding fluid from an initial starting position to its point of impact (upper vane).

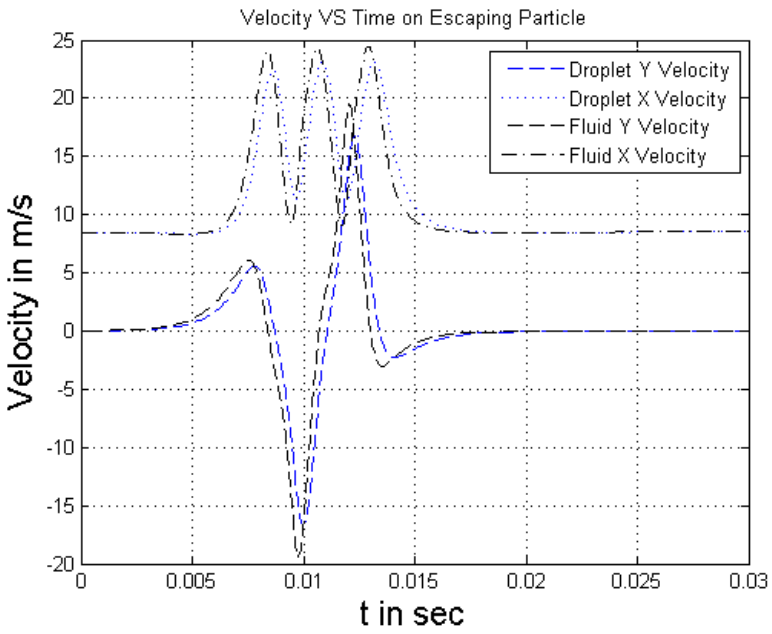

Shown above is the velocity profile with respect to time of a droplet (contaminant), and the surrounding fluid from an initial starting position which has escaped the demister.